Supplementary Material

Competition between water uptake and ice nucleation by glassy organic aerosol particles

T. Berkemeier[1,2], M. Shiraiwa[1], U. Pöschl[1] and T. Koop[2,*]

[1] Multiphase Chemistry Department, Max Planck Institute for Chemistry, Mainz, Germany

[2] Faculty of Chemistry, Bielefeld University, Bielefeld, Germany

Correspondence to: T. Koop (thomas.koop@uni-bielefeld.de)

1. Treatment of gas diffusion

To account for local depletion of trace gases in the near-surface gas phase of aerosol particles acting as a sink for the respective gases, Shiraiwa et al. (2012) use a gas phase diffusion correction factor for species Z, $C_{g,Z}$, as described previously by Pöschl et al. (2007). In this formalism a corrected near-surface trace gas concentration $[Z]_{gs}$ is obtained through the uptake coefficient of Z, γ_Z, and the Knudsen number Kn_Z of the diffusion system. Since the trace gas uptake γ_Z itself depends on $[Z]_{gs}$ and thus via $C_{g,Z}$ on its own value, this formalism significantly increases the stiffness of the set of differential equations that needs to be solved. In the new formalism, a different approach of gas phase diffusion correction is employed. The approach assumes a gaseous shell with a thickness of one mean free path λ_Z around the particle as well, but treats all mass fluxes to and from this shell explicitly in a separate differential equation. In particular, the diffusion flow $F_{net,Z}$ from this far-surface gas phase into the near-surface gas shell can be calculated as diffusion through a virtual particle envelope with $d_p + 2\,\lambda_Z$ diameter (Pöschl et al., 2007). Applying Fick's first law yields

$$\boldsymbol{F}_{\mathbf{net,g,Z}} = \boldsymbol{4\pi}\left(\boldsymbol{r}_{\mathbf{p}} + \boldsymbol{\lambda}_{\mathbf{Z}}\right)\boldsymbol{D}_{\mathbf{g,Z}}\left([\mathbf{Z}]_{\mathbf{g}} - [\mathbf{Z}]_{\mathbf{gs}}\right). \quad \text{(S1)}$$

Since in all calculations that we performed, particle size was approximately on the order of the mean free path, we chose the respective limiting case for calculation of the mean free path $\boldsymbol{\lambda}_{\mathbf{Z}}$ differently from Pöschl et al. (2007) by using Eq. (S2) as given in Seinfeld and Pandis (2006) and valid for $d_p \approx \lambda_Z$.

$$\lambda_Z = \frac{1.7\, D_{g,Z}}{\omega_Z} \tag{S2}$$

2. Physico-chemical parameterizations

In the following sections we list all physico-chemical parameterizations employed in this study. For simulations of the sucrose/water model system, we use parameterizations for density, water activity and bulk diffusivity by Zobrist et al. (2011). Glass transition values are taken from Zobrist et al. (2008), gas diffusivities of water from Winkler et al. (2006), while vapor pressures of ice and water are taken from Murphy and Koop (2005). A few miscellaneous model parameters are compiled in Table S2.

2.1. Density

For the sucrose/water system density can be parameterized as a function of the organic weight fraction w_{org} with a fourth-order polynomial function (Zobrist et al., 2011).

$$\rho_{tot}(w_{org}) = a_0 + a_1 w_{org} + a_2 w_{org}^2 + a_3 w_{org}^3 + a_4 w_{org}^4 \tag{S3}$$

where $a_0 = 0.9989$, $a_1 = 0.3615$, $a_2 = 0.2964$, $a_3 = -0.3186$ and $a_4 = 0.24191$.

For all other systems, volume additivity was assumed, leading to the following expression of density as function of w_{org} and density ρ_{org} of the pure compounds.

$$\rho_{tot}(w_{org}) = \frac{1}{(1 - w_{org}) + \frac{w_{org}}{\rho_{org}}} \tag{S4}$$

2.2. Water activity

For the determination of water activity from composition data, several different approaches are used. For sucrose and levoglucosan, parameterizations from Zobrist et al. (2011) and Zobrist et al. (2008) are used, respectively. In these parameterizations, water activity is described as function of temperature and organic weight fraction as follows:

$$a_w(T, w_{org}) = \frac{1 + a w_{org}}{1 + b w_{org} + c w_{org}^2} + (T - T^{\ominus})(d w_{org} + e w_{org}^2 + f w_{org}^3 + g w_{org}^4) \tag{S5}$$

Parameters for these two substances are given in Table S4. For substances for which no previous parameterization was available, we employ Kappa-Koehler theory, using the single hygroscopicity parameter κ_{org} or the equivalent van't Hoff parameter i_{org} to determine water activity (Petters and Kreidenweis, 2007).

$$a_w(w_{org}) = \frac{1}{1 + \frac{\kappa_{org}}{\rho_{org}} \cdot \frac{w_{org}}{1 - w_{org}}} = \frac{1}{1 + i_{org} \cdot \frac{M_w}{M_{org}} \frac{w_{org}}{1 - w_{org}}} \quad \text{(S6)}$$

For citric acid, a composition-dependent fit of i_{org} has been provided by Koop et al. (2011).

$$i_{org} = 1 + 2.1408 w_{org}^2 \quad \text{(S7)}$$

Lienhard et al. (2012) give an alternative parameterization that behaves differently especially at lower temperatures (cf. Figure). We note however that at T < 220 K we use the parameterization outside of its validity range. The functional form of this parameterization is given in Eq. (S8) and parameters given in Table S5.

$$\begin{aligned} a_w &= \frac{1 - w_{org}}{1 + q \cdot w_{org} + r \cdot w_{org}^2} \\ q &= a_1 + a_2 T + a_3 T^2 \\ r &= a_4 + a_5 T + a_6 T^2 \end{aligned} \quad \text{(S8)}$$

2.3. Bulk diffusivity

Bulk diffusivity of water in the aqueous organic mixtures, D_{H2O}, is parameterized using a (modified) Vogel-Fulcher-Tammann (VFT) approach that uses three parameters to account for its super-Arrhenius dependence on temperature (Vogel, 1921;Fulcher, 1925;Tammann and Hesse, 1926).

$$D_{H2O}(T, a_w) = 10^{-\left(A(a_w) + \frac{B(a_w)}{T - T_0(a_w)}\right)} \quad \text{(S9)}$$

Here, T_0 is the so-called Vogel temperature, indicating the temperature at which D_{H2O} goes to zero. T_0 is closely related to the Kauzmann temperature, T_k, that is the hypothetical point where the entropy of amorphous and crystalline solid would coincide, which is often referred to as the "Kauzmann paradox" (Kauzmann, 1948;Stillinger, 1988). Parameter A can be regarded as the high temperature maximum of water diffusivity ($T >> T_0$), whereas B represents the steepness of the viscous slowdown, the so-called *fragility* (Angell, 1985, 1995). According to Angell (1985), a liquid with low B exhibits *fragile* character, indicating a strong deviation of the temperature dependence from Arrhenius behaviour. Liquids with high B on the other hand (e.g. network formers such as SiO_2) show the typical Arrhenius behaviour and are classified as *strong* liquids.

Zobrist et al. (2011) provided a set of water activity-dependent fit functions for the sucrose/water system based on experimental data over a wide temperature and concentration range.

$$\boldsymbol{A(a_\mathrm{w}) = 7 + 0.175\big(1 - 46.46(1 - a_\mathrm{w})\big)} \tag{S10}$$

$$\boldsymbol{B(a_\mathrm{w}) = 262.867(1 + 10.53(1 - a_\mathrm{w}) - 0.3(1 - a_\mathrm{w})^2)} \tag{S11}$$

$$\boldsymbol{T_0(a_\mathrm{w}) = 127.9(1 + 0.4514(1 - a_\mathrm{w}) - 0.5(1 - a_\mathrm{w})^{1.7})}. \tag{S12}$$

2.4. Glass transition

In a binary system glass transition temperatures of mixtures can be described as a function of w_org by the Gordon-Taylor equation (Gordon and Taylor, 1952), using the glass transition temperature of the pure components ($T_\mathrm{g,H2O}$ and $T_\mathrm{g,org}$) and the Gordon-Taylor coefficient k_GT:

$$\boldsymbol{T_\mathrm{g}\big(w_\mathrm{org}\big) = \frac{\big(1 - w_\mathrm{org}\big)\,T_\mathrm{g,w} + \frac{1}{k_\mathrm{GT}} w_\mathrm{org} T_\mathrm{g,org}}{\big(1 - w_\mathrm{org}\big) + \frac{1}{k_\mathrm{GT}} w_\mathrm{org}}} \tag{S13}$$

The component with the lower glass transition temperature, in this case water, acts as a plasticizer, decreasing the glass point of the mixture with decreasing weight fraction w_org.

2.5. Gas phase diffusivity

The gas phase diffusion coefficient of water can be obtained using the temperature and pressure dependent parameterization provided in Winkler et al. (2006),

$$\boldsymbol{D_\mathrm{g,H2O}(T, p) = 1.9545\, T^{1.6658}\, p^{-1}}. \tag{S14}$$

2.6. Vapor pressures of ice and water

Above 110 K, the vapor pressure of hexagonal ice is parameterized according to Murphy and Koop (2005) as

$$\boldsymbol{p_\mathrm{ice}(T) = \exp 9.550426 - \frac{5723.265}{T} + 3.53068 \ln T - 0.00728332\, T}. \tag{S15}$$

For the vapor pressure of water, Murphy and Koop provided

$$\ln p_{\mathrm{liq}}(T) = 54.842763 - \frac{6763.22}{T} - 4.210 \ln T + 0.000367\, T + \tanh[0.0415(T - 218.8)] \left(53.878 - \frac{1331.22}{T} - 9.44523 \ln T + 0.014025\, T\right) \quad \text{(S16)}$$

for temperatures between 123 K and 332 K. Both parameterizations have been used in this study.

Supporting Tables

Table S1. SOA marker substances used to estimate water diffusivities and estimated melting point and glass transition values.

Name	Structure	M (g mol-1)	T_m, est./(lit.) (K)	T_g, est. (K)
A-PINENE				
C107OOH	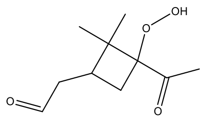	200.231	320.01	224.01
PINONIC	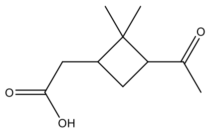	184.232	349.60 (378.65)	244.72
C97OOH	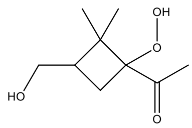	188.221	346.31	242.41
C108OOH	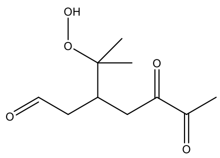	216.231	323.83	226.68
C89CO2H	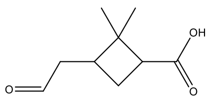	170.206	348.78	244.15
PINIC	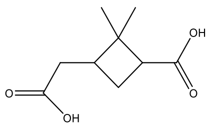	186.205	420.30 (355)	294.21
C921OOH	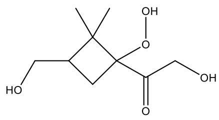	204.220	367.19	257.03
C109OOH	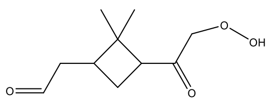	200.231	298.17	208.72
C812OOH	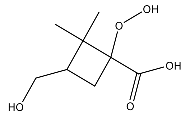	190.194	441.53	309.07

HOPINONIC	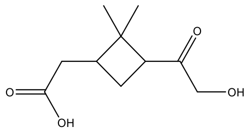	200.232	371.25	259.88
C811OH	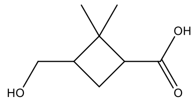	158.094	380.32	266.22
C813OOH	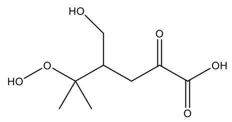	206.193	548.31	383.81
ALDOL_dimer	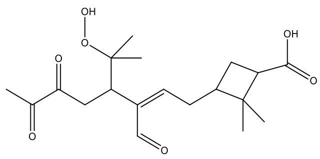	368.421	391.59	274.11
ESTER_dimer	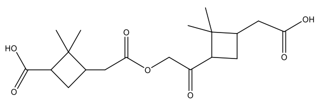	368.421	424.07	296.85
pinonaldehyde	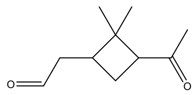	168.23	278.08	194.65
terpenylic acid	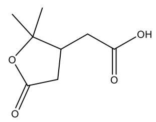	172,17	433.1	303.66
2-hydroxy terpenylic acid	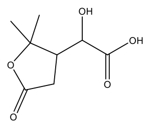	188,17	524.57	367.20
diaterpenylic acid acetate	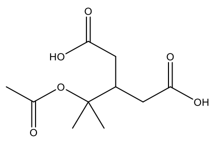	232,22	391.86	274.31
3-MBCTA	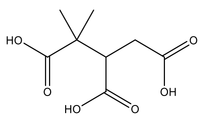	204.177	480.26	336.18
ISOPRENE				
C_5 alkene triol (aldol form)	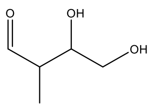	118.127	304.68	213.28
C_5 alkene triol (keto form)	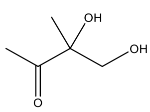	118.127	346.16	242.31

2-methyltetrol	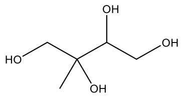	136.142	404.73	283.31
C_5 trihydroxy acid	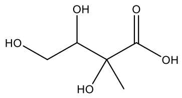	150.125	441.04	308.73
hemiacetal dimer	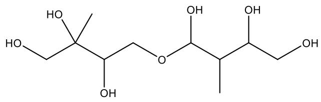	254.269	407.63	285.34
methyltetrol performate	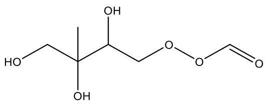	180.15	393.30	275.31
2-methylglyceric acid	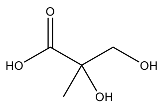	120.1	416.87	291.81
2-MG/mono- acetate dimer	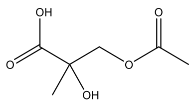	162.14	381.46	267.02
2-MG/2-MG dimer	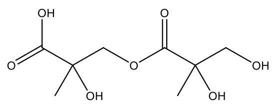	222.185	475.66	332.96
$(2\text{-MG})_3$ trimer	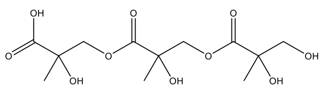	324.27	500.75	350.52
$(2\text{-MG})_4$ tetramer	…	426.355	516.47	361.53
NAPHTHALENE				
Kautzman122/ benzoic acid	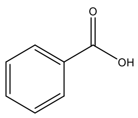	122.116	384.80 (395.5)	269.36*
Kautzman138	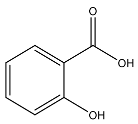	138.115	459.00 (431.75)	321.30*
Kautzman166/ phthalic acid	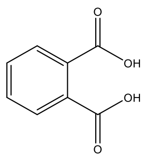	166.124	538.92 (403.15 decomp.)	377.25*
1-Hydroxy-naphthalene	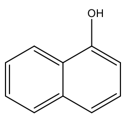	144.170	362.87 (368.15)	257.71*

2-Hydroxy-naphthalene	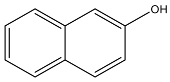	144.170	362.87 (394.65)	276.26*
1,2-naphthalene-dione	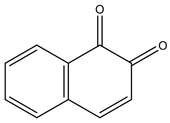	158.154	457.35 (419.15)	293.41*
1,4-naphthalene-dione	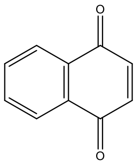	158.154	457.35 (401.65)	281.16*
2-Hydroxy-1,4-naphthalenedione	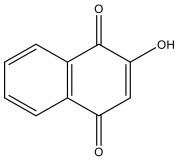	174.153	533.47 (468)	327.60*
5-Hydroxy-1,4-naphthalenedione	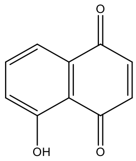	174.153	396.32 (428)	299.60*
Kautzman192/ 2-carboxy-cinnamic acid	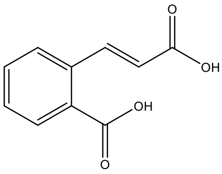	192.171	561.06 (473.15)	331.21*
DODECANE				
CARB	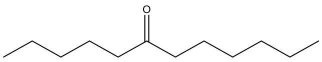	184.31	272.12	190.48
THF derivative	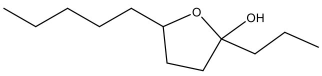	200.31	368.27	257.79
CARBROOH	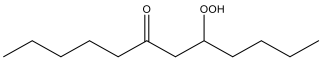	216.31	311.74	218.22
OHDICARB	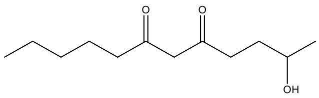	214.29	284.36	199.05
Peroxydiol1	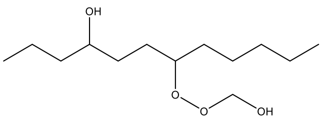	248.35	307.59	215.31
Peroxydiol2	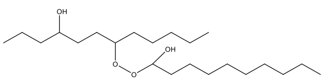	374.58	326.45	228.51

Peroxyketone1	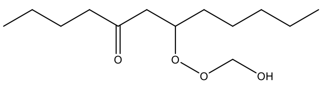	246.33	285.74	200.02
Peroxyketone2	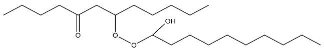	386.59	329.43	230.60
OHCARBROOH	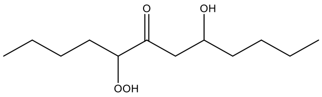	232.31	314.74	220.32
CnACID C7H14O3	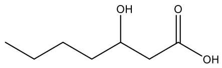	146.18	328.47	229.93
Zhang299	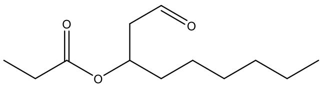	214.29	270.86	189.60
Zhang301	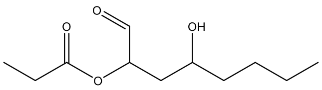	216.27	296.82	207.77
Zhang315	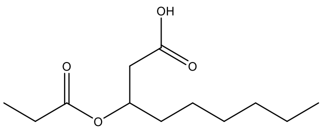	230.29	308.34	215.84

*: Glass point estimated from literature melting point.

Table S2. Full list of upper temperature limits (in K) for heterogeneous ice nucleation.

SOA Class	**O/C**	**Lower estimate**	**Best guess**	**Upper estimate**
A-PINENE	0.3	207.48	212.56	217.69
	0.5	213.20	217.46	221.88
	0.7	215.80	220.90	225.96
ISOPRENE	0.6	202.43	210.67	218.73
	0.8	206.21	211.99	218.10
	1.0	206.28	213.28	220.38
NAPHTHALENE	0.3	223.06	226.06	229.09
	0.5	219.21	223.27	227.37
	0.7	216.08	221.46	226,72
DODECANE	0.1	211.79	215.73	219.55
	0.3	205.69	209.29	213.15
	0.5	199.12	204.92	211.10

Table S3. Various model parameters.

$T_{g,H2O}$ (K)	$a_{s,0}$ ()	$\tau_{D,H2O}$ (s)	ρ_{SOA} (g cm^{-3})	M_{SOA} (g mol^{-1})
136	1	4e-11	1.4	250

Table S4. Parameters for water activity parameterization, Eq. (S5).

Substance	a	b	c	d	e	f	g
Sucrose	–1	–0.99721	0.13599	0.001688	–0.005151	0.009607	–0.006142
Levoglucosan	–0.99918	–0.90978	0.021448	0.00045933	0.0035813	0.00026549	0.0033059

Table S5. Parameters for water activity parameterization, Eq. (S8), after Lienhard et al. (2012).

Substance	a_1	a_2	a_3	a_4	a_5	a_6
Citric acid	−3.16761	0.01939	−4.02725e-5	6.59108	−0.05294	1.06028e−4

Supporting Figures

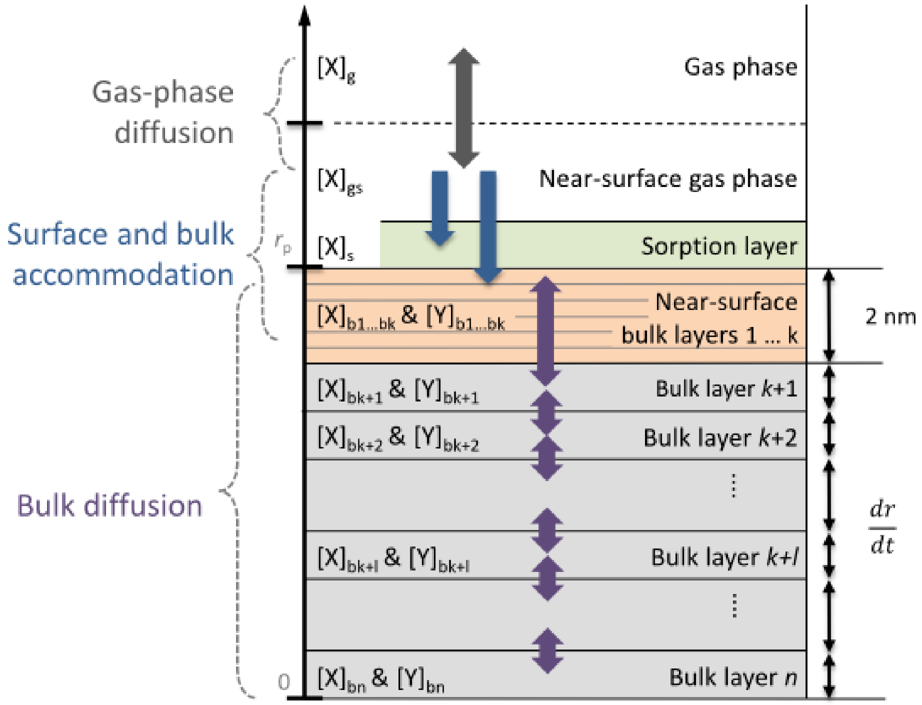

Figure S1. Schematic of KM-GAP and key mass transport processes including gas-phase diffusion (grey arrow), accommodation (blue arrow) and bulk diffusion (purple arrows). The near-surface bulk (orange box) has been resolved finely with *k* layers to keep track of a 1 nm surface region that is crucial for formation of an initial ice embryo in immersion freezing scenarios. All *n* bulk layers are allowed to grow and shrink.

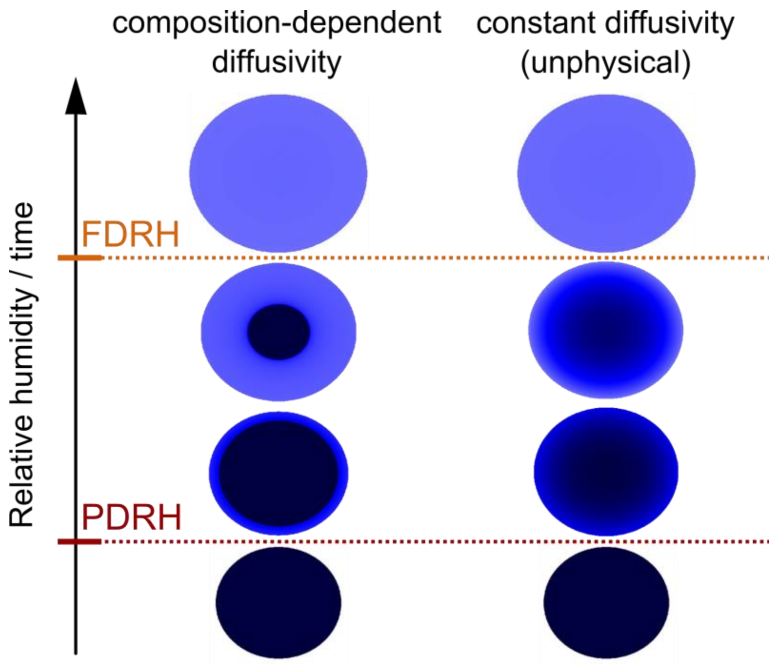

Figure S2. Schematic evolution of particle morphology upon humidification in two different scenarios. In the left column, diffusivity depends on water content and the liquefaction process is characterized by a sharp diffusion front moving into the particles. For comparison, the right column shows an unrealistic case of water diffusing into the particle with constant diffusivity.

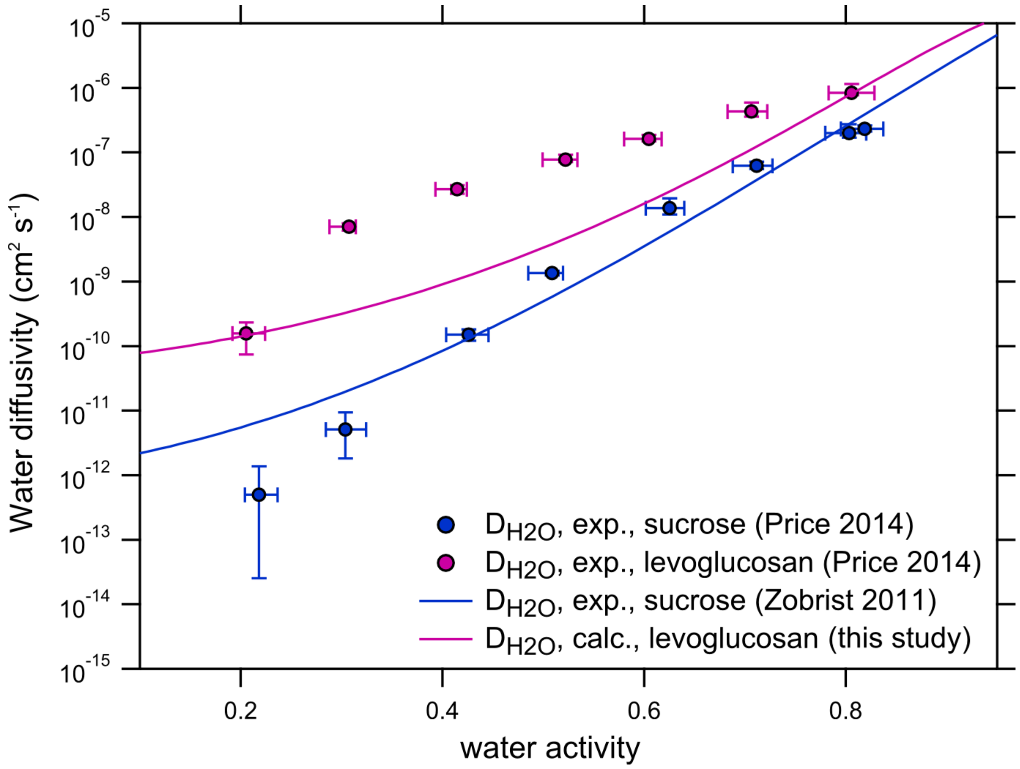

Figure S3. Comparison of estimated water diffusivities with experimental results for water in sucrose and levoglucosan matrices as measured by Price et al. (2014). The D_{H2O} for sucrose parameterized by Zobrist et al. (2011) is in good agreement with the observations, except for the different curvature that leads to deviations for low RH. D_{H2O} in levoglucosan is higher than D_{H2O} in sucrose, which is captured by the method proposed in this study. The curvature remains different since the predicted D_{H2O} in levoglucosan is only inferred from sucrose data.

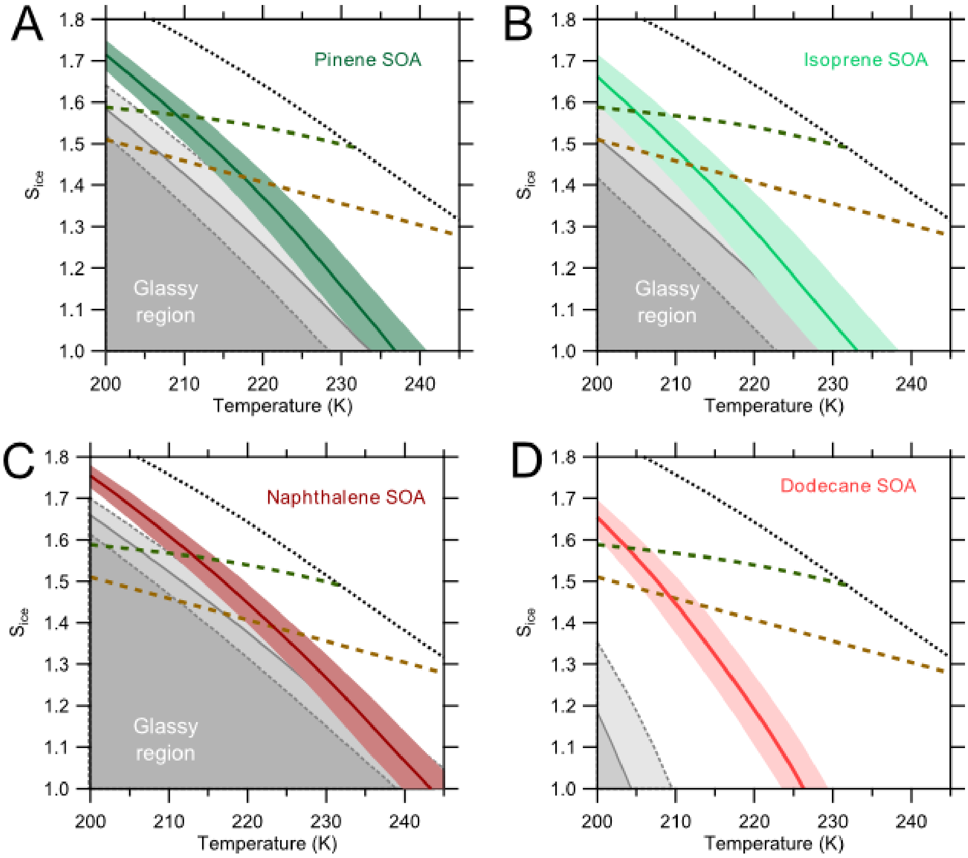

Figure S4. Quasi-equilibrium (RH_g, grey lines) and kinetic (FDRH, coloured lines) glass transition values of the four SOA precursor classes (A) a-pinene, (B) isoprene, (C) naphthalene, and (D) dodecane. Uncertainty in quasi-equilibrium glass transition is given by dashed lines and grey shades, the uncertainty in FDRH is shown as shaded bands in the respective colour. Naphthalene SOA shows the highest glass transition values whereas dodecane SOA shows the lowest, in agreement with experiments by Saukko et al. (2012).

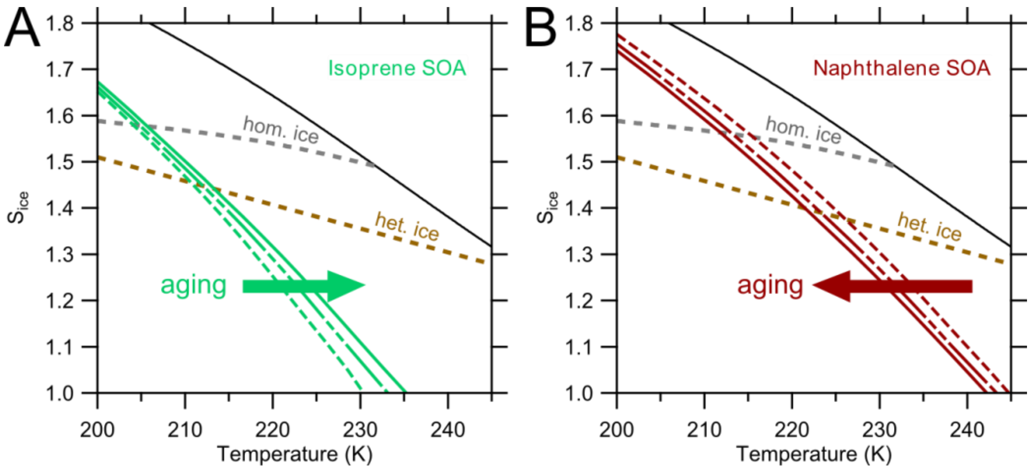

Figure S5. Effect of particle ageing on full deliquescence relative humidity (FDRH, solid and dashed lines) for (A) isoprene and (B) naphthalene SOA. Isoprene SOA shows slight hardening upon increase in O/C (indicated by higher FDRH), whereas Naphthalene SOA exhibits slight softening (indicated by lower FDRH).

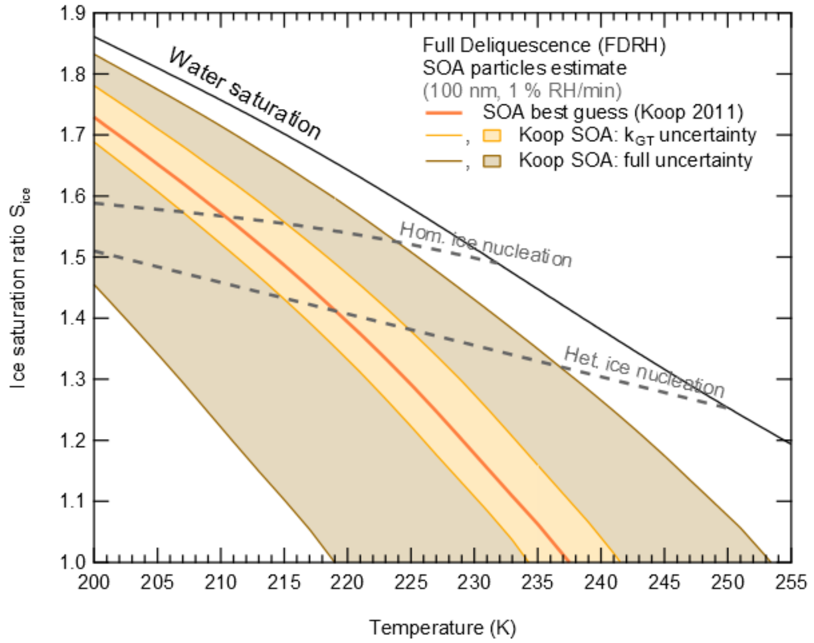

Figure S6. Results of deliquescence experiments (100 nm particles, humidified at a rate of 1 % RH min^{-1}, starting at S_{ice} = 1) using the diffusivity estimation scheme for the SOA best guess parameters of Koop et al. (2011). The uncertainty arising from uncertainty in k_{GT} is shown as the orange shaded area; the overall uncertainty arising from uncertainty in all input parameters (κ_{org}, $T_{g,org}$ and k_{GT}) is shown as the grey shaded area.

Supporting Movies

Movie S1. Simulation of humidification of a 200 nm sucrose particle from 60 % to 95 % RH at 215 K at a rate of 1 % RH min^{-1}. Water activity of the particle and ambient RH (left bottom corner) are colour-coded from dark blue (low a_w /RH) to light blue (high a_w /RH).

Movie S2. Simulated humidification of a 200 nm sucrose particle from 60 % to 95 % RH at 215 K under the unphysical assumption that water diffusivity does not change with water content and instead was fixed to $5 \cdot 10^{-14}$ cm^2 s^{-1}. The employed humidification rate is 1 % RH min^{-1}. Water activity of the particle and ambient RH (left bottom corner) are colour-coded from dark blue (low a_w /RH) to light blue (high a_w /RH).

References

Angell, C. A.: in: Relaxations in Complex Systems, edited by: Ngai, K., and Wright, G. B., National Technical Information Service, I.S. Department of Commerce, Springfield, VA, 1985.

Angell, C. A.: Formation of glasses from liquids and biopolymers, Science, 267, 1924-1935, 1995.

Fulcher, G. S.: Analysis of recent measurements of the viscosity of glasses, J. Am. Ceram. Soc., 8, 339-355, 10.1111/j.1151-2916.1925.tb16731.x, 1925.

Gordon, M., and Taylor, J. S.: Ideal copolymers and the 2nd-order transitions of synthetic rubbers. 1. Non-crystalline copolymers, J. Appl. Chem., 2, 493-500, 1952.

Kauzmann, W.: The nature of the glassy state and the behavior of liquids at low temperatures, Chem. Rev., 43, 219-256, 10.1021/cr60135a002, 1948.

Koop, T., Bookhold, J., Shiraiwa, M., and Pöschl, U.: Glass transition and phase state of organic compounds: dependency on molecular properties and implications for secondary organic aerosols in the atmosphere, Phys. Chem. Chem. Phys., 13, 19238-19255, 2011.

Lienhard, D. M., Bones, D. L., Zuend, A., Krieger, U. K., Reid, J. P., and Peter, T.: Measurements of Thermodynamic and Optical Properties of Selected Aqueous Organic and Organic-Inorganic Mixtures of Atmospheric Relevance, J. Phys. Chem. A, 116, 9954-9968, 10.1021/jp3055872, 2012.

Murphy, D. M., and Koop, T.: Review of the vapour pressures of ice and supercooled water for atmospheric applications, Q. J. R. Meteorol. Soc., 131, 1539-1565, 10.1256/qj.04.94, 2005.

Petters, M. D., and Kreidenweis, S. M.: A single parameter representation of hygroscopic growth and cloud condensation nucleus activity, Atmos. Chem. Phys., 7, 1961-1971, 2007.

Pöschl, U., Rudich, Y., and Ammann, M.: Kinetic model framework for aerosol and cloud surface chemistry and gas-particle interactions - Part 1: General equations, parameters, and terminology, Atmos. Chem. Phys., 7, 5989-6023, 2007.

Price, H. C., Murray, B. J., Mattsson, J., O'Sullivan, D., Wilson, T. W., Baustian, K. J., and Benning, L. G.: Quantifying water diffusion in high-viscosity and glassy aqueous solutions using a Raman isotope tracer method, Atmos. Chem. Phys., 14, 3817-3830, 10.5194/acp-14-3817-2014, 2014.

Saukko, E., Lambe, A. T., Massoli, P., Koop, T., Wright, J. P., Croasdale, D. R., Pedernera, D. A., Onasch, T. B., Laaksonen, A., Davidovits, P., Worsnop, D. R., and Virtanen, A.: Humidity-dependent phase state of SOA particles from biogenic and anthropogenic precursors, Atmos. Chem. Phys., 12, 7517-7529, 10.5194/acp-12-7517-2012, 2012.

Seinfeld, J. H., and Pandis, S. N.: Atmospheric chemistry and physics - From air pollution to climate change, John Wiley & Sons, Inc., New York, 2006.

Shiraiwa, M., Pfrang, C., Koop, T., and Pöschl, U.: Kinetic multi-layer model of gas-particle interactions in aerosols and clouds (KM-GAP): linking condensation, evaporation and chemical reactions of organics, oxidants and water, Atmos. Chem. Phys., 12, 2777-2794, 10.5194/acp-12-2777-2012, 2012.

Stillinger, F. H.: Relaxation and flow mechanisms in fragile glass-forming liquids, J. Chem. Phys., 89, 6461-6469, 10.1063/1.455365, 1988.

Tammann, G., and Hesse, W.: The dependancy of viscosity on temperature in hypothermic liquids, Z. Anorg. Allg. Chem., 156, 14, 1926.

Vogel, H.: The temperature dependence law of the viscosity of fluids, Physik. Z., 22, 645-646, 1921.

Winkler, P. M., Vrtala, A., Rudolf, R., Wagner, P. E., Riipinen, I., Vesala, T., Lehtinen, K. E. J., Viisanen, Y., and Kulmala, M.: Condensation of water vapor: Experimental determination of mass and thermal accommodation coefficients, J. Geophys. Res. Atmos., 111, D19202, 10.1029/2006jd007194, 2006.

Zobrist, B., Marcolli, C., Pedernera, D. A., and Koop, T.: Do atmospheric aerosols form glasses?, Atmos. Chem. Phys., 8, 5221-5244, 2008.

Zobrist, B., Soonsin, V., Luo, B. P., Krieger, U. K., Marcolli, C., Peter, T., and Koop, T.: Ultra-slow water diffusion in aqueous sucrose glasses, Phys. Chem. Chem. Phys., 13, 3514-3526, 10.1039/c0cp01273d, 2011.